

*Rapid communication***Structure in the angular dependence of optical suppression of photoassociative ionization collisions within an optically cooled and collimated sodium atom beam**W. DeGraffenreid^{1,*}, J. Ramirez-Serrano¹, Y.-M. Liu^{1,**}, R. Napolitano², A. Rosenbaum^{1,***}, J. Weiner^{3,****}¹Laboratory for Atomic, Molecular, and Optical Science and Engineering, University of Maryland College Park, MD 20742, USA²IFSC, Universidade de São Paulo, São Carlos, SP 13560-970, Brazil³IRSAMC/LCAR, Université Paul Sabatier, 118 route de Narbonne, 31062 Toulouse, France

Received: 9 June 2000/Revised version: 21 September 2000/Published online: 8 November 2000 – © Springer-Verlag 2000

Abstract. We report measurements of the angular distribution of optical suppression in photoassociative ionization collisions taking place within a bright, slow Na atom beam. At a collision “temperature” ($T = E_{\text{kin}}/k_B$) of about 5 mK we observe rich structure in the suppression measure as a function of the angle between the atom-beam axis and the polarization axis of the suppressor light beam. This structure cannot be explained by the superposition of individual partial-wave contributions to the suppression measure, and we propose a partial-wave interference phenomenon to account for it.

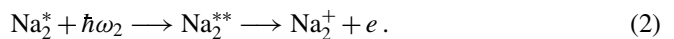
PACS: 07.77.Gx; 32.80.Pj; 32.80.Lg

The three attributes of light fields – intensity, frequency, and polarization – can manipulate atomic interactions and control the outcome of inelastic or reactive collisions. Optical cooling of atoms to submillikelvin temperatures and their confinement in optical and magnetic traps led to an early proposal [1] to study photoassociation in ultracold binary collisions between sodium atoms by imposing an optical field red-detuned with respect to the atomic resonance transition. Since then numerous theoretical and experimental investigations [2] have developed the physics of precision photoassociation spectroscopy, the results of which have in turn led to highly accurate determinations of molecular potentials, atomic lifetimes, scattering lengths, and the production of ultracold molecules. These studies complement molecular beam laser spectroscopy determination of the last bound levels that have recently been performed [3]. The rate of ionization from a two-stage process, photoassociative ionization

(PAI) [4, 5], provides a sensitive probe of the photoassociation rate. The first step is photoassociation itself,



followed by the absorption of a second photon to a doubly excited state that subsequently autoionizes,



Detuning ω_1 to the red of the atomic resonance transition while holding ω_2 fixed generates a photoassociation spectrum in the Na_2^+ ion signal.

Optical fields blue-detuned with respect to the atomic resonance transition can also be used to suppress photoassociation and shield atoms from mutual short-range interaction. The suppression field ω_S couples the incoming scattering flux to long-range repulsive molecular states, effectively preventing the atoms from approaching close enough to undergo any strong-interaction inelastic or reactive process.



Strong-field models of optical suppression [6, 7] have predicted a striking modulation of the suppression probability as a function of the angle between the polarization of the suppressor field and the atomic collision axis. Experiments in magneto-optical traps (MOTs) [2] are not sensitive to these effects because the molecular axis averaged over all collisions is spatially isotropic. However, collisions within a highly collimated atom beam, in which the molecular collision angle is greatly restricted, will reveal angular structure. A recent beam experiment [8] showed evidence for this angular anisotropy, but the intensity of the scattering flux was not sufficient to measure a detailed angular dependence of the suppression probability.

In a new experiment, using transverse optical cooling to increase atom-beam brightness by a factor of 4×10^4 , we report the observation of a surprisingly rich structure in the angular distribution of optical suppression in PAI at a collision energy of about 5 mK. Figure 1 shows a schematic layout of the apparatus.

*Present address: Physics Laboratory, National Institute of Standards and Technology, Gaithersburg, MD 20899, USA

**Present address: Department of Modern Applied Physics, Tsinghua University Beijing 100084, China

***Present address: Department of Chemistry, University of Chicago, Chicago, IL 60697, USA

****Corresponding author.

(Fax: +33-561/558-317, E-mail: jweiner@yosemite.ups-tlse.fr)

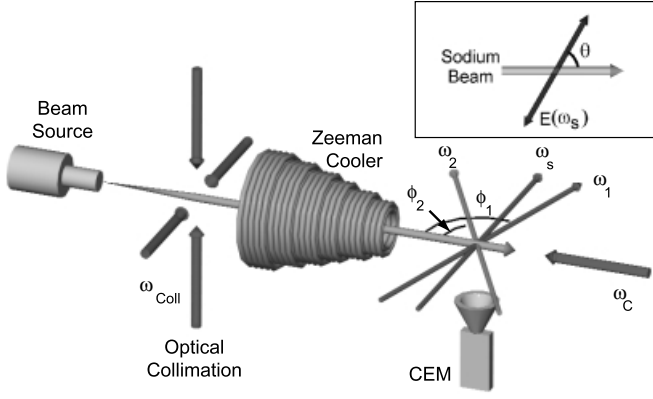


Fig. 1. Schematic of the apparatus showing the atom-beam source, optical cooling of transverse velocity components, Zeeman cooler for axial velocity cooling, and the disposition of $\omega_1, \omega_2, \omega_s$ with respect to the atom beam. *Inset* shows the angle between the polarization axis of ω_s (propagating into the page) and the sodium beam

1 Experiment

A heated metal vapor oven furnishes a flux of sodium atoms which is collimated by a skimmer and injected into a coaxial tapered-solenoid Zeeman cooler. An annular liquid nitrogen trap and several coils of water-cooled refrigeration tube, both concentric with the atom-beam axis, together with a small diffusion pump remove vapor rejected by the skimmer structure. Just prior to injection into the Zeeman cooler a “lin-perp-lin” arrangement of two pairs of counterpropagating laser beams, orthogonal to each other and to the atom beam, optically cools the transverse velocity components v_x, v_y to submillikelvin temperatures, thereby creating a highly collimated atom flux. At the collisional interaction zone, 1.8 m downstream from the Na source, optical collimation increases the atom density n from 1×10^7 to $3 \times 10^8 \text{ cm}^{-3}$, the beam solid angle divergence ($\Omega = \pi v_{x,y}^2 / v_z^2$) reduces from 1.8×10^{-4} to $1.3 \times 10^{-7} \text{ sr}$, and the atom-beam brightness ($B = n/\Omega$) increases from 5.6×10^{10} to $2.3 \times 10^{15} \text{ cm}^{-3} \text{ sr}^{-1}$, a factor of 4.1×10^4 . Light from a ring dye laser ω_c , tuned about 220 MHz to the red of the $^2S(F=2) \rightarrow ^2P(F=3)$ cycling transition and counterpropagating to the atom beam, cools a fraction of the atomic v_z thermal distribution. Near the exit of the Zeeman cooler a small cylindrical fixture wrapped with 15 turns of high-magnetic-permeability metal foil abruptly cuts off the magnetic field gradient and decouples the atom beam from the optical cooling transition. The magnetic-shield fixture is adjusted at a point near the end of the cooler so as to maximize the intensity and minimize the velocity dispersion of the decelerated atoms [8]. Abrupt decoupling from ω_c also prevents optical pumping of the slowed atoms into the $F=1$ ground state hyperfine level. The atom beam subsequently enters a field-free interaction zone where three light fields labeled $\omega_1, \omega_2, \omega_s$ intersect the atom beam at a common point. Figure 1 shows the disposition of the atom beam carrying the cooled velocity group and the three light fields. The two light beams ω_1, ω_2 induce PAI collisions within the narrow velocity group by the usual two-step process described by (1) and (2) with detunings of 370 MHz to the red and 555 MHz to the blue of the cycling transition, respectively. These detunings refer to the moving coordinate frame of the cooled velocity

group. Figure 1 also shows the angular offset of ω_1, ω_2 with respect to the z axis. These offsets angle-tune the two PAI optical beams to excite only the cooled velocity group and discriminate against unwanted ionization signals coming from collision of background or other velocity classes of the sodium jet. Using a weak probe laser beam sweeping over the resonance transition and traversing the atom beam at an angle of about 60° , we record the Doppler- and power-broadened atomic fluorescence line shape. From a fit of this line shape to a Voigt profile, we extract the axial component of the atomic laboratory velocity distribution $p_a(v)$. Figure 2 shows this fit for typical experimental conditions.

The relative axial collision velocity distribution $p_{\text{col}}(v_r)$ derives from the autocorrelation of the atomic velocity distribution $p_a(v)$ for each atom in the binary collision with $v_r = |v_1 - v_2|$,

$$p_{\text{col}}(v_r) = \int_0^\infty dv_1 \int_0^\infty dv_2 p_a(v_1) p_a(v_2) \delta(v_r - |v_1 - v_2|). \quad (4)$$

The distribution $p_{\text{col}}(v_r)$ is plotted in the inset of Fig. 2. The average relative collision velocity is then calculated from

$$\langle v_r \rangle = \int_0^\infty p_{\text{col}}(v_r) v_r dv_r. \quad (5)$$

We take the definition of the “temperature” of the intra-atom-beam collisions to be

$$\frac{1}{2} \mu \langle v_r \rangle^2 = k_B T, \quad (6)$$

with μ being the reduced mass of the colliding atoms and k_B the Boltzmann constant. Applying (4), (5) and (6) to the data in Fig. 2 results in a collision temperature of about 5 mK. The light beam ω_s , tuned 270 MHz to the blue of the cy-

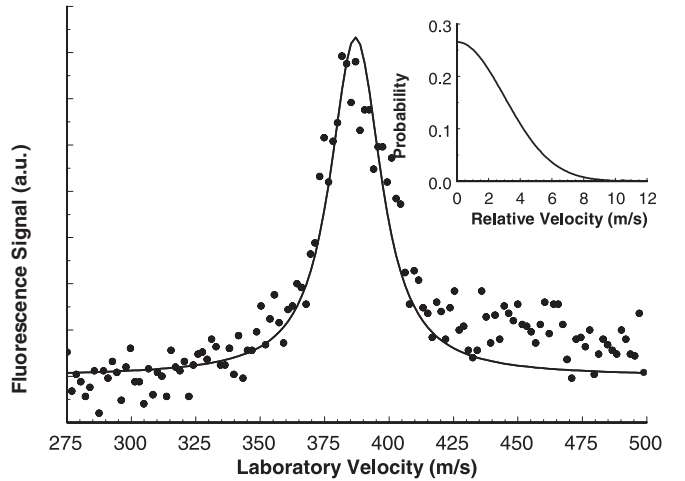


Fig. 2. Fit of atom-beam fluorescence spectrum to the Voigt profile. The line shape has been mapped into velocity space and includes power broadening from the probe laser. The velocity distribution is obtained from the Voigt fit. *Inset* shows relative probability distribution calculated from (4)

clinging transition, intersects the atom beam at right angles and optically couples the colliding pairs to a manifold of hyperfine long-range repulsive molecular levels. A mechanical chopper interrupts ω_1 at 150 MHz and provides the external timing signal for a two-channel gated particle counter (Stanford Research Instruments model SR400). Ions are detected on a channel-electron-multiplier (Dr. Sijts model KBL 25RS) mounted vertically below the horizontal plane containing the optical and atom beams and centered on the vertical axis running through their intersection point. Channel A counts ions with ω_1 and ω_2 present; channel B counts ions with ω_1 blocked by the mechanical chopper. The PAI signal is the difference between channels A and B. We adapt the term “shielding measure” from [6] and determine a “suppression measure” by recording the PAI signal i with the suppression field ω_S present (i_S) and absent (i_0) and taking the ratio of the two ionization rates:

$$P_S(\theta, I_S) = \frac{i_S}{i_0}. \quad (7)$$

This ratio was recorded as a function of the angle θ between the ω_S polarization axis and the atom-beam axis over a range from $0 - 180^\circ$ and at two suppressor beam intensities, I_S : one low ($I_S = 0.6 \text{ W cm}^{-2}$) and one high ($I_S = 2.5 \text{ W cm}^{-2}$). We note that optical pumping of the Na atoms out of the $F = 2$ ground state by ω_S would result in a spurious suppression signal. Taking into account detuning, power density, and dwell time in the interaction zone ($\simeq 2.5 \mu\text{s}$), we estimate an upper limit of no more than 10% for this effect. Figure 3a shows polar plots of P_S at the two suppression field intensities, and Fig. 3b shows the same data on a linear plot with the error bars ($\pm\sigma$).

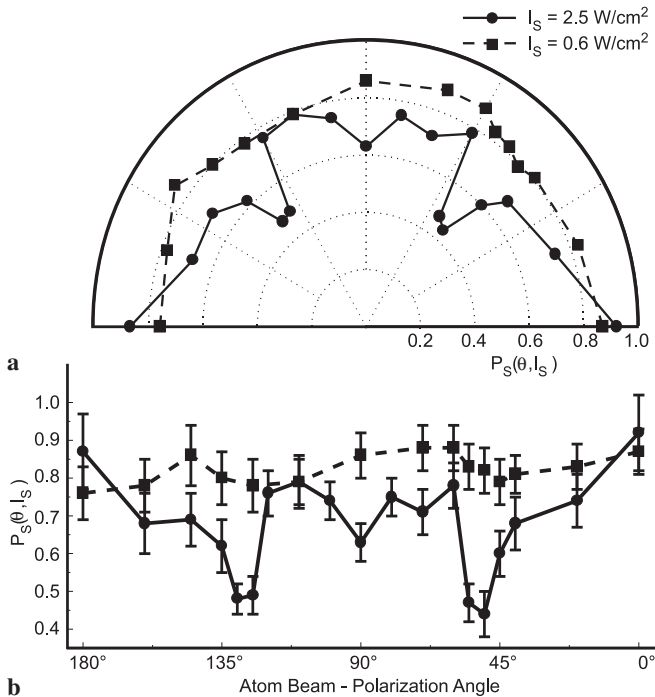


Fig. 3. **a** Polar plot of $P_S(\theta, I_S)$ at two suppressor beam intensities, 0.6 W cm^{-2} and 2.5 W cm^{-2} . **b** Same data plotted on $x - y$ coordinates showing error bars ($\pm\sigma$)

2 Result

At low suppression intensity ($I_S = 0.6 \text{ W cm}^{-2}$) the angular distribution is isotropic, but at high field ($I_S = 2.5 \text{ W cm}^{-2}$) the angular plot exhibits pronounced dips in P_S at about 55° and 125° , with a small dip at 90° . The two-step process, in which the initial excitation (1) occurs at very long range ($\simeq 560 a_0$) and the autoionization at short range ($\simeq 3 a_0$), restricts the effective acceptance angle of the PAI event to a narrow cone of about 6 mrad around the molecular axis. Together with the very small angular divergence of the atom beam in the laboratory frame ($\simeq 1.6 \text{ mrad}$), this assures that the molecular collision axis aligns closely with the laboratory atom-beam axis [8]. Therefore angular variation in the optical suppression probability measured in the laboratory frame with respect to atom-beam axis tracks closely the angular behavior of optical suppression in the molecular collision frame.

Optical suppression of photoassociative ionization was first reported in experiments carried out in a MOT and interpreted in terms of a one-dimensional Landau-Zener optically dressed potential crossing (LZ-1D) model [9]. Later experiments [10, 11] revealed the inadequacy of the LZ-1D picture. The experiments showed that the suppression effect saturated with increasing intensity at ω_S and that circular polarization was much more effective than linear polarization. Similar saturation behavior was observed in ultracold collisions of metastable xenon atoms [12, 13] and metastable krypton atoms [14]. Failure of the LZ-1D model motivated the development of a three-dimensional quantum close coupling (QCC-3D) model [6] with a more exact treatment of the strong-field regime. In this model, angular structure arises from contributions of individual partial waves to the final exit collision channel and from possible interferences among them. A three-dimensional multiple-crossing Landau-Zener (LZ-3D) model has also been advanced by Yurovsky and Ben-Reuven [7]. Their approach preserves the curve crossing picture on a manifold of dressed molecular potentials, each member of which is associated with a scattering partial wave. The LZ-3D picture interprets angular structure in the optical suppression to arise from interfering scattering flux on these different partial-wave potentials, leading to the same final PAI channel. Although previous model calculations [6, 7] predicted intensity-dependent angular structure in P_S , it could always be identified as a dominant contribution to the PAI exit channel from one partial wave. The present results cannot be interpreted so easily, however, since the structure does not correspond to any dominating d, g, i, \dots partial wave, but may be due to quantum interference between two or more partial waves. Using a highly accurate sodium dimer ground-state triplet potential [15], scattering calculations show that a d -wave shape resonance occurs in the vicinity of 5 mK collision energy [16]. The combination of the scattering resonance and the multiple pathways leading from the same entrance to exit channels may then produce an interference structure in the suppression measure. In support of this conjecture, Fig. 4 shows two calculated polar plots of the suppression measure under conditions similar to those of the high intensity case of the experiment and based on the QCC-3D model [6, 17]: one (dashed line, peak at 90°) corresponds to an incoherent addition of the partial wave contributions, while the other (solid line, dip around 90°) results from a coherent addition.

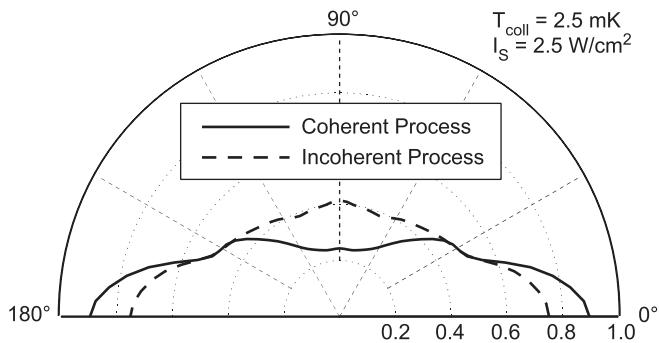


Fig. 4. Calculations of $P_S(\theta, I_S)$ based on the model of [6]. The polar plots show a thermal average at 2.5 mK and a suppressor laser intensity of 2.5 W cm^{-2} , similar to the experimental conditions. *Dashed curve* shows the result of an incoherent superposition of partial wave contributions. *Solid curve* shows the result for a coherent superposition. The model calculation for the low intensity case shows an isotropic suppression measure that has been described in detail elsewhere [6]

Comparing the experimental (Fig. 3) and theoretical (Fig. 4) patterns, one immediately sees that the coherent addition of partial waves, exhibiting a dip around 90° , results in a calculated angular distribution closer to the measured one. This “agreement”, however, is at best qualitative; the very simple five-state, spinless model calculation ignores much of the complexity in the real collision engendered by spin-orbit and hyperfine angular momentum coupling. Earlier studies [11] have shown that this model demonstrates qualitatively the polarization and intensity dependence of the suppression measure, but is not adequate for a quantitative description. Therefore we conclude that the qualitative comparison of the calculated and measured angular distributions supports the presence of a partial wave interference but

a more elaborate multistate calculation may be necessary to confirm it.

Acknowledgements. Support from the National Science Foundation, the Army Research Office, and the National Institute of Standards and Technology is gratefully acknowledged.

References

1. H.R. Thorsheim, J. Weiner, P.S. Julienne: *Phys. Rev. Lett.* **58**, 2420 (1987)
2. J. Weiner, V.S. Bagnato, S. Zilio, P.S. Julienne: *Rev. Mod. Phys.* **71**, 1 (1999); This reference provides a recent list of citations to the vast literature of ultracold collisions
3. M. Elbs, H. Knöckel, T. Laue, C. Samuelis, E. Tiemann: *Phys. Rev. A* **59**, 3665 (1999)
4. P.L. Gould, P.D. Lett, P.S. Julienne, W.D. Phillips, H.R. Thorsheim, J. Weiner: *Phys. Rev. Lett.* **60**, 788 (1988)
5. R.W. Heather, P.S. Julienne: *Phys. Rev.* **47**, 1887 (1993)
6. R. Napolitano, J. Weiner, P.S. Julienne: *Phys. Rev. A* **55**, 1191 (1997)
7. V.A. Yurovsky, A. Ben-Reuven: *J. Phys. Chem. A* **102**, 9476 (1998)
8. C.-C. Tsao, Y. Wang, R. Napolitano, J. Weiner: *Eur. Phys. J. D* **4**, 139 (1998)
9. L. Marcassa, S. Muniz, E. de Queiroz, S. Zilio, V. Bagnato, J. Weiner, P.S. Julienne, K.-A. Suominen: *Phys. Rev. Lett.* **61**, 935 (1994)
10. L. Marcassa, R. Horowicz, S. Zilio, V. Bagnato, J. Weiner: *Phys. Rev. A* **52**, R913 (1995)
11. S.C. Zilio, L. Marcassa, S. Muniz, R. Horowicz, V. Bagnato, R. Napolitano, J. Weiner, P.S. Julienne: *Phys. Rev. Lett.* **76**, 2033 (1996)
12. M. Walhout, U. Sterr, C. Orzel, M. Hoogerland, S.L. Rolston: *Phys. Rev. Lett.* **74**, 506 (1995)
13. K.-A. Suominen, K. Burnett, P.S. Julienne, M. Walhout, U. Sterr, C. Orzel, M. Hoogerland, S.L. Rolston: *Phys. Rev. A* **53**, 1658 (1996)
14. H. Katori, F. Shimizu: *Phys. Rev. Lett.* **73**, 2555 (1994)
15. E. Tiesinga, C.J. Williams, K.M. Jones, P.D. Lett, W.D. Phillips: *J. Res. Nat. Inst. Stand. Technol.* **101**, 505 (1996)
16. E. Tiesinga: private communication
17. R. Napolitano: private communication